LU TP 95-12
June 1995
revised

Discrete QCD, A New Approximation for QCD Cascades

B. Andersson [1], G. Gustafson [2], J. Samuelsson [3]

Department of Theoretical Physics
Lund University
Sölvegatan 14A
S-223 62 Lund, Sweden

Abstract

We consider a new approximation scheme to the perturbative QCD cascades, Discrete QCD, corresponding to an expansion in the phase space density of the emitted partons. It turns out that this density in phase space is very low and the reason can be traced to the physics behind the running coupling constant. The whole scheme only contains a single parameter, *viz* the scale in the running coupling constant and is consequently strongly predictive. We show how to obtain analytical formulas for the multiplicity and the phase space distributions and compare to the results of the conventional cascade models (JETSET, ARIADNE and HERWIG) as well as earlier analytical approximation schemes.

[1] bo@thep.lu.se (internet)
[2] gosta@thep.lu.se(internet)
[3] jim@thep.lu.se (internet)

1 Introduction

In order to be able to compare the results of basic theory to the very complex high energy experiments performed today it is necessary to develop theoretical models for eg multigluon emission. (At present there is in general precise results only available up to the next to leading order in the coupling constant). There are several such models, which are based upon perturbative approximations to the basic QCD equations. It is of interest to investigate exactly the reasons why some particular schemes work well, eg those expressed as Monte Carlo simulation schemes in JETSET [1], ARIADNE [2]and HERWIG [3], while others do not. One essential ingredient for a succesful approximation is to take the coherence properties of the gluonic radiation into account and it is also necessary to be able to "stop" the cascades in an infrared stable manner. It is generally difficult, however, to provide closed analytical formulas for the observables.

In this note we develop a new approximation method to the cascades, inside which it is easy to obtain analytical formulas and in which there is a definite simple cutoff in the cascades. We have called it Discrete QCD because phase space is in the model partitioned into finite cells, each one containing a single effective gluon emission. Although the phase space for the emission of a particular gluon depends upon the prehistory of the cascade ("the phase space is growing" which is tantamount to the statement that QCD exhibits "anomalous dimensions") there is for a given total energy only a finite number of emissions possible.

In order to describe the scheme we will start (Section 2) with an introduction to the perturbative cascades and in particular dwell on the properties of the Dipole Cascade Model (DCM) which is at the basis of ARIADNE. We will also compare to the conceptually very different scheme of the Webber-Marchesini model as described in HERWIG. This is done also to show the properties of the QCD Coherent Bremsstrahlung Phase Space. After that we will in section 3 consider the properties of the running coupling constant in QCD and show that it implies that the phase space density of the emitted partons is very low. In particular in the space of $(\log(k_\perp^2), y)$ there is a typical distance between the emitted gluons of the order of $11/6 \sim 2$ units.

We will consider this result as a definition of the Discrete QCD Model (cf Section 4), ie *we will partition phase space into cells of that size.* We show the consequences, in particular that the running coupling constant in this way "arranges" the probability density to be constant in the growing phase space. Further all the relative probabilities can be expressed in terms of rational numbers and we note that the model contains only a single parameter, the scale of the running coupling constant. As an example we calculate both the distributions in phase space size and in the multiplicity.

We show in Section 5 a set of scaling properties (depending both upon the absolute energy scale and the resolution scale). We will also briefly exhibit the zeroes in the complex plane of the generating function for the multiplicities, [4]. These zeroes describe in a precise way all the moments of the distribution. We find that it constitutes a Julia set in mathematical language, ie all zeroes have a finite distance from the origine but together they build up a fractal curve of the same beauty and complexity as eg the Mandelbrot set. The relationship to the scaling properties mentioned before is not known.

In order to make comparisons with experimental data for more complex distributions we introduce in section 6 a simple Monte Carlo. This Monte Carlo generates events with parton momenta, taking into account appropriate recoils etc. As examples we show some results for the thrust distribution.

2 The Dipole Cascade Model versus the Webber-Marchesini Cascades

2.1 The DCM

In order to describe the properties of the Discrete QCD Model we will provide a brief introduction to the properties of perturbative QCD multigluon cacscades. We will in this note work inside an e^+e^--annihilation scenarium in which an initial (color singlet) $q\bar{q}$-state is formed. This state will at high energies emit gluons by color dipole radiation in accordance with the well-known formula:

$$dP = \frac{C\alpha_S}{2\pi} dx_1 dx_3 \frac{(x_1^2 + x_3^2)}{(1-x_1)(1-x_3)} \tag{1}$$

Here C is a color factor ($C = 4/3$ for a $q\bar{q}$-dipole), α_s the coupling constant and x_j the cms energy fractions of the final state partons with the emitted gluon x_2 fulfilling

$$x_2 + x_1 + x_3 = 2 \tag{2}$$

We note in passing that the mass squares of the parton pairs (qg) ($s_{12} = W^2(1-x_3)$) and $(g\bar{q})$ ($s_{23} = W^2(1-x_1)$) are expressible in terms of the original dipole mass W and the x_j's.

It is convenient to introduce the Lorentz invariant transverse momentum and rapidity

$$\begin{aligned} k_\perp^2 &\equiv W^2(1-x_1)(1-x_3) \\ y &\equiv \frac{1}{2}\log\left(\frac{1-x_1}{1-x_3}\right) \end{aligned} \tag{3}$$

and in terms of these variables we have for the cross section ($x_1 \simeq x_3 \simeq 1$)

$$dP \simeq \frac{C\alpha_s}{\pi}\frac{dk_\perp^2}{k_\perp^2} dy \tag{4}$$

For the phase space we have in the cms of the dipole

$$k_\perp \cosh(y) \leq \frac{W}{2} \tag{5}$$

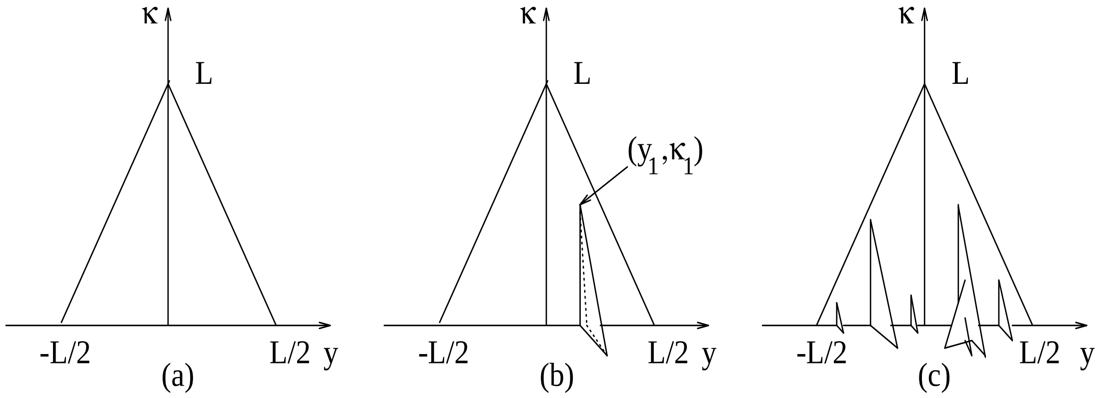

Figure 1: *(a) The phase space available for a gluon emitted by a high energy $q\bar{q}$ system is a triangular region in the y-κ plane. (b) If one gluon is emitted at (y_1, κ_1) the phase space for a second (softer) gluon is represented by the area of this folded surface. (c) Each emitted gluon increases the phase space for the softer gluons. The total gluonic phase space can be described by this multifaceted surface.*

which can be conveniently approximated by

$$k_{\pm} \equiv k_{\perp} \exp(\pm y) < W \tag{6}$$

corresponding to a triangular region in the $(y, \kappa \equiv \log(k_{\perp}^2))$-plane, cf fig 1a.

The formula is besides the color factor the same as the one obtained in QED but in this case there is a major change in the final state. Emitting a photon in QED does not change the current but in QCD the emitted gluon is an octet and therefore the final state contains a color 3 (the q), an $\bar{3}$ (the $\bar{q}$) and the 8-gluon. There is, however, the simplification that instead of forming a complex charge system, the three final state partons form *two independent dipoles*, [5]. Thus if we consider the emission of two gluons, indexed 1 and 2, where $k_{\perp 1} \geq k_{\perp 2}$, the cross section is factorisable into

$$dP(q\bar{q} \to qg_1g_2\bar{q}) = dP(q\bar{q} \to qg_1\bar{q})\{dP(qg_1 \to qg_2g_1) + dP(g_1\bar{q} \to g_1g_2\bar{q})\} \tag{7}$$

where all the terms dP on the right hand side have the form given in eq (4). This factorisation property is better than a few percent all over the phase space, [6]. We note in particular that $k_{\perp}$ and y in the dipole emission terms are defined in the rest frame of the particular dipole, which for the softer gluons differs from the original cms.

The DCM is then based upon the production of one dipole $\to$ two dipoles $\to$ three...etc, [7]. Every time a new gluon is emitted the corresponding dipole is partitioned. Actually the final state containing a set of dipoles has a strong similarity to the Lund String with a set of gluon excitations dragging out a set of straight string segments (corresponding to the dipoles), cf fig 2. As the masses of the dipoles quickly diminish, the corresponding gluons quickly become soft. A general rule in string fragmentation is that a gluon with less than a few GeV of transverse momentum does no longer really produce any noticeable effects. Therefore adding to the cascade the use of Lund string fragmentation means that the whole process is infrared stable.

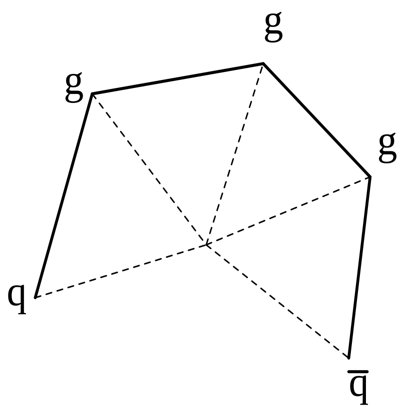

Figure 2: *The dipoles connect the quarks and gluons in the same way as the string in the Lund string fragmentation model.*

It is useful to note that one gluon emission actually increases the phase space for further emissions. While the cms rapidity region, Δy, available for the first gluon emission is $\log(W^2/k_{\perp 1}^2)$ the two independent new dipoles may emit inside a total range

$$(\Delta y)_{gen} = \log(s_{12}/k_{\perp 2}^2) + \log(s_{23}/k_{\perp 2}^2) = \log(W^2/k_{\perp 2}^2) + \log(k_{\perp 1}^2/k_{\perp 2}^2) \tag{8}$$

where in the last expression we have used the lines after eq (2) and eq (3). Consequently there will by the emission be an increase, $\delta y = \log(k_{\perp 1}^2/k_{\perp 2}^2)$, and this can be conveniently "added" to the triangular phase space in fig 1a by extending a (double) fold as in fig 1b. Actually we are in this way adding a triangular region, made up of the two sides of the fold, to the original triangle.

It is easy to see that each new emission has the same effect on the phase space. After several emissions we obtain a complex figure with many folds "sticking out" as in fig 1c. The length of the baseline, called λ, is given by the expression

$$\sum \log(s_{i,i+1}) = \log(W^2) + \sum \log(k_{\perp i}^2) \tag{9}$$

It can be interpreted as an effective rapidity range for the final produced hadrons and is strongly correlated to the hadron multiplicity, [8, 9]. The baseline is irregular and behaves like a (multi)fractal with the so-called anomalous dimension of QCD basically equal to the fractal dimensions, [10, 11].

2.2 Comparison to the Webber-Marchesini Cascades

So how come that the Lund Model and the Webber-Marchesini Model (corresponding to emission along the individual parton lines instead of building dipoles), which are conceptually so different nevertheless will lead to so similar predictions (with very good agreement to the LEP-data)? *The building of dipoles in the cascade is actually the same as the requirement of angular ordering in the emissions*, [12]. Consequently, the two different cascades developing along different lines nevertheless cover the same phase space region of fig 1c. In the dipole scheme it is searched from top to bottom, while in the Webber-Marchesini scheme it is searched sideways going from a central angle or rapidity out towards the ends.

In order to see this we note that Webber-Marchesini use one angular variable, θ, and one energy variable, E. Remembering the relationship between the rapidity of a massless particle ("pseudo-rapidity" for all others):

$$y = \frac{1}{2}\log\left(\frac{e+p_l}{e-p_l}\right) = -\log(\tan(\theta/2)) \simeq -\log(\theta/2) \tag{10}$$

and the approximate relation $k_\perp \simeq E\theta$ we may map these variables onto the quantities $(y, k_\perp)$ and consider the emission of a Webber-Marchesini cascade in the triangular phase space. The strong angular ordering means that after emitting a "first" gluon along a parton line (emission angle θ) the next emission must have an emission angle smaller than θ and so on. This means that in this kind of cascade you may start with a first emission at some angle or rapidity and then afterwards go towards the q-end in rapidity (ie following the emissions along the q-line) and afterwards go towards the $\bar{q}$-end in rapidity (ie following along the $\bar{q}$-line).

In both cases the "new" emissions are evidently fulfilling the angular ordering requirement (ie diminishing angles along the parton line). In every "step" in rapidity one searches through the possible $k_\perp$- (or E)-values, ie one "goes from one side in rapidity, y, towards the other, all the time looking up and down in $k_\perp$". Every time one finds an emission a "new" parton line starts out and *this corresponds exactly to adding a folded triangle* in the Lund language. Then they are searched through in the same manner, producing subfold triangles etc.

According to our description above, one is in the Lund DCM "going down in $k_\perp$ all the time looking left and right inside the relevant rapidity region", also adding folds and resolving them for new emissions. If all the gluons were strongly ordered the two schemes would give the same result, but in reality recoils and other nonleading effects cause some differences. Here perturbative QCD does not give a clear answer because in these regions interference effects are important and the probabilistic cascade does not give an exact description.

To give a complete description of an event, the parton cascade must be complemented with a hadronization model. In the end of the cascade Bryan Webber has introduced a "cluster" fragmentation scheme. In this way he builds chains of decaying clusters along the same regions where the Lund String is spanned and breaks up

3 The Properties of the Running Coupling Constant

The density of gluons is (besides the color factor) governed by the running coupling constant in QCD. It is well-known that the change from a constant to a running coupling means that certain higher order corrections are accounted for in the calculations. It is also well-known that these corrections stem from the introduction of what in field theory is known as the "vertex" and "self-energy" corrections. In a more intuitive language it means that we take into account the *polarisability properties of the vacuum*, ie the fact that a newly produced gluon will be surrounded by a set of virtual partons, which can be emitted and absorbed. In that way the vacuum occurs as a dielectric medium and this will influence the color force fields and their excitations.

In order to demonstrate more precisely these properties we consider a scale-change in the way we define a field quantum and its interaction. This means that the field operator, normalised to a single quantum at one scale, will be changed and the same goes for the coupling constant, which likewise has been normalised in the renormalisation procedure at this scale. These changes can be read out from the Callan-Symanzik equations so that a quantity $\mathcal{M}$ will vary with the scale μ^2 according to

$$\mu^2 \frac{\partial \mathcal{M}}{\partial \mu^2} + \beta \frac{\partial \mathcal{M}}{\partial \alpha} - \gamma \mathcal{M} = 0 \tag{11}$$

The β-part stems from the change in the coupling constant and the γ-part ("the anomalous dimensions") from the field operator normalisation change.

This kind of equations are known all over physics (as well as in other disciplines) as gain-loss-equations and eg Coleman gave in his Erice lectures, [13], an example with $\mathcal{M}$ corresponding to the size of a bacteria population, moving with a fluid along a pipe. One follows the development in "the time" $\log(\mu^2)$. The fluid has a velocity β with α a coordinate along the pipe and as they move along there is a changing illumination γ, which determines their rate of reproduction. A positive β-term would in the terminology of gain-loss-equations correspond to a "loss" when the "time" $\log(\mu^2)$ increases (and a negative β likewise a loss when $\log(\mu^2)$ decreases).

In case we neglect all other scales (like restmasses etc) it is in a renormalisable field theory simple to prove that both β and γ are functions only of the coupling constant. The β-term in QCD can be written as

$$-\beta \frac{\partial \mathcal{M}}{\partial \alpha} = \left(\frac{11}{6}\frac{3\alpha_s}{2\pi} - \frac{2}{3}\frac{n_f \alpha_s}{4\pi}\right) \alpha_s \frac{\partial \mathcal{M}}{\partial \alpha_s} \tag{12}$$

The formula is written in this way in order to exhibit "the loss properties" when the scale decreases. We firstly note that in case $\mathcal{M}$ corresponds to a multigluon emission amplitude then the quantity

$$\alpha_s \frac{\partial \mathcal{M}}{\partial \alpha_s} \equiv N(\mathcal{M}) \tag{13}$$

is a measure of the multiplicity of the (already) emitted gluons. The coupling constants

$$\frac{3\alpha_s}{2\pi} \equiv \bar{\alpha}(g \to gg) \quad \text{and} \quad \frac{n_f \alpha_s}{4\pi} \equiv \bar{\alpha}(g \to q\bar{q}) \tag{14}$$

are the relevant ones for a gluon splitting into either a gluon pair or a $q\bar{q}$-pair (and therefore also for the corresponding reverse processes when the pairs go back to a gluon, ie are "reabsorbed").

Finally the two quantities

$$\delta y_g = \frac{11}{6} \quad \text{and} \quad \delta y_q = \frac{2}{3} \tag{15}$$

are just the typical rapidity regions for these two processes, respectively.

To see that we consider a situation when a few gluons have been emitted in a DCM scenarium. We focus on one of the dipoles with the mass W, spanned between two such gluons. As the cascade develops we will according to the rules "go downwards" in $k_\perp$, ie the scale $\log(k_\perp^2) \equiv \kappa$ decreases. A gluon can be emitted if the gluon rapidity according to eq (5) is limited by $|y| < \log(W/k_\perp)$.

A closer examination, however, exhibits that there is a region close to endpoints of the dipole where there is a depletion of emitted gluons, [14], (taking this correction into account means in the business language of perturbative QCD that one would go from the Leading Log to the Modified Leading Log approximation, cf [12]). The effective rapidity range depends upon the charge at the endpoint but for a (gg)-dipole it is $\log((W/k_\perp)^2) - 11/6$ in the limit when $W \to \infty$.

The border of the dipole is just the (earlier) emitted gluon (and there is another dipole "on the other side" of that gluon). Therefore *in the neighbourhood of an already emitted gluon there is a region of loss* equal to δy_g when we go downwards in the DCM. If this statement is rephrased from dipole language to "diagrammatic language" it would be: In case a highly virtual gluon (virtuality corresponds to the dipole mass W) decays into a gluon pair with given $k_\perp$ then the reverse process, ie reabsorption, will effectively take place in case the two gluons are inside the rapidity region $\delta y_g = 11/6$.

In even more detail, the total rapidity region for emission of a pair with $\pm\vec{k}_\perp$ contains both the part $\log((W/k_\perp)^2)$ (this is a particular feature of vector emission, in which the quantas can spread very far and which in non-abelian gauge theories is compensated by the vertex corrections —or else they would not have been renormalisable) and $-11/6$. The reason why one has such a spreading of vector quantas is directly related to helicity conservation, ie a spin 1/2-quantum emitting a vector should keep its helicity and therefore the vector must be emitted "softly" with a z-pole. Similarly a vector decaying into two vectors cannot in order to keep its helicity allow both of them to move "closely" to its original direction and therefore the probability distribution contains both a z- and $(1-z)$-pole. This means that as $dz/z(1-z) = dz(1/z + 1/(1-z))$ and dz/z (or $dz/(1-z)$) equals dy there is no other damping than energy conservation for large y. For $g \to (q\bar{q})$ however, the vector gluon "would like" the two fermions to be "parallell", ie there are no poles in this decay distribution. The whole marvel is the fact that nonabelian gauge theories are renormalisable at all.

Thus when the vector decays into a fermion pair, the splitting function contains no z-pole and consequently *there is for the $(q\bar{q})$-pair an exponential suppression of large rapidities.* This means that we have a finite effective rapidity region for emission (and absorption) which becomes $\delta y_q = 2/3$ (and no renormalisation at all is necessary here).

In this way we may interpret the β-function as the probability to reabsorb any emitted pair (whether gluons or $(q\bar{q})$), ie *any pair going closer together in rapidity than the above-described δy will effectively be reabsorbed.* This is at the origin of the running coupling constant in QCD:

$$\alpha_s = \frac{12\pi}{33 - 2n_f} \frac{1}{\log(k_\perp^2)} \tag{16}$$

which is the solution to the differential equation

$$k_\perp^2 \frac{d\alpha_s}{dk_\perp^2} = \beta(\alpha_s) \tag{17}$$

We note that in case we introduce $\kappa = \log(k_\perp^2)$ and let the number of flavors, n_f vanish (ie we neglect the gluon splitting into $(q\bar{q})$-pairs — this is only a correction of the order of a few percent in any cascade) we have for the effective coupling in eq (14)

$$\bar{\alpha}(g \to gg) = \frac{1}{\delta y_g \cdot \kappa} \tag{18}$$

Thus the probability to emit a gluon from a (gg)-dipole (in the same approximation as in eq (4)) can be written in the form

$$dP = \frac{dy d\kappa}{\delta y_g \cdot \kappa} \tag{19}$$

a result which we will use below.

4 The Discrete QCD Model

We have found that there is a typical rapidity difference necessary between gluons. If two gluons are closer than the size $\delta y_g = 11/6 \sim 2$ then they will effectively be reabsorbed into a single gluon again. We will then assume that all "effective" gluons, ie all those which will not be absorbed again, must have a "distance" corresponding to δy_g. Thus the rapidity range is separated in windows with width δy_g and all the gluons emitted in such a window will act coherently as one effective gluon. The momentum of this effective gluon ought to be well approximated by the *hardest* of all gluons emitted in this rapidity window.

From eq (19) we find the distribution in $\kappa = \log(k_\perp^2)$ of gluons within the j:th bin with width δy_g

$$dP(j, \kappa) = \frac{d\kappa}{\delta y_g \cdot \kappa} \delta y_g = \frac{d\kappa}{\kappa} \tag{20}$$

Therefore the distribution of the *effective* gluon is given by

$$dProb(j,\kappa) = dP(j,\kappa)\exp[-\int_{\kappa}^{\kappa_{max}} dP(j,\kappa')] \tag{21}$$

where we have introduced the exponential Sudakov formfactor (which in probability language means that no emission has occurred between the largest transverse momentum allowed for the rapidity y_j and the one we consider). Evaluating the integral in the exponent gives the simple result

$$dProb(j,\kappa) = \frac{d\kappa}{\kappa_{max}} \tag{22}$$

In this way we obtain inside any "step" δy_g the same probability to emit an effective gluon for any value of κ (we note that κ_{max} depends upon which rapidity step we are considering).

Consider in the spirit of the Webber-Marchesini model the emission of gluons! Then it will be necessary to take finite steps in rapidity, corresponding to δy_g, ie we emit "effective" gluons, which cannot be reabsorbed in the future stages of the cascade. The probability in the step j to obtain a particular emission is given by eq (21).

Emitting a gluon means according to our earlier discussion also adding a folded triangle. In case we go into this triangle and want to emit again we find by the same requirement that also the steps in κ must be "quantised" into an (even) integer times δy_g and the same goes for the subfold triangles etc. The reason for an even integer is that all folds contains two sides with each side corresponding to the color and anticolor of the emitted gluon.

A little reflection tells us that this pattern with an "original baseline", correponding to the $(q\bar{q})$-dipole, with two-sided trees emerging out of it (corresponding to the "first" generation of gluons), each one able to send out (two-sided) branches, containing in turn (two-sided) "twigs" and "sprigs" etc, (for an example cf fig 3) is the most general way to describe any color connected bremsstrahlung pattern stemming from an original singlet ($3\bar{3}$). The distances between the neighbouring "tips" correspond to the logarithm of the squared dipole masses.

In that way a particular event, corresponding to a triangle with baseline $\log(W^2) = L \cdot \delta y_g$, ($L$ =integer) contains a "grove" of trees, with the maximal tree-lengths $j \cdot \delta y_g$, where $j = 1, 2 \ldots j_{max}$ with $j_{max} = L/2$ if L is even and $j_{max} = (L-1)/2$ if L is odd. If the maximal tree-height is $j \cdot \delta y_g$ the actual height is given by one of the values $l \cdot \delta y_g$, where $l = 0, 1 \ldots j$ with equal probabilities for the possible values. To simplify later relations, we will call such a tree a "true N-tree", with $l = N-1$ and it corresponds to an emitted (effective) gluon with $\log(k_\perp^2) = \kappa = 2l \cdot \delta y_g$. For a tree with maximal height $(N-1) \cdot \delta y_g$, we introduce the notation "free N-tree", which thus corresponds to a mixture of true M-trees, with equal probabilities for $M = 1, \ldots, N$, as discussed above. The notions of a true N-tree and a free N-tree are illustrated in fig 4.

The model is now fully specified. Each event corresponds to a diagram of the type shown in fig 3, with probabilities as discussed above. This diagram determines the rapidity and transverse

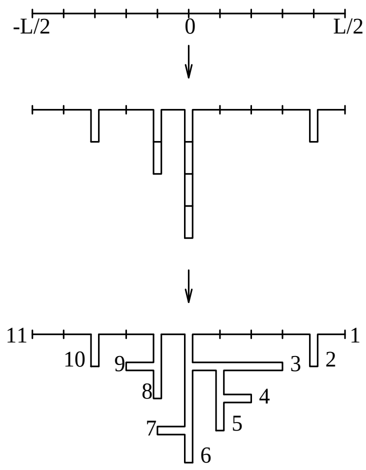

Figure 3: *Evolution of branches in the tree structure from the original straight baseline (the $q\bar{q}$ dipole), through a number of gluon emissions. .*

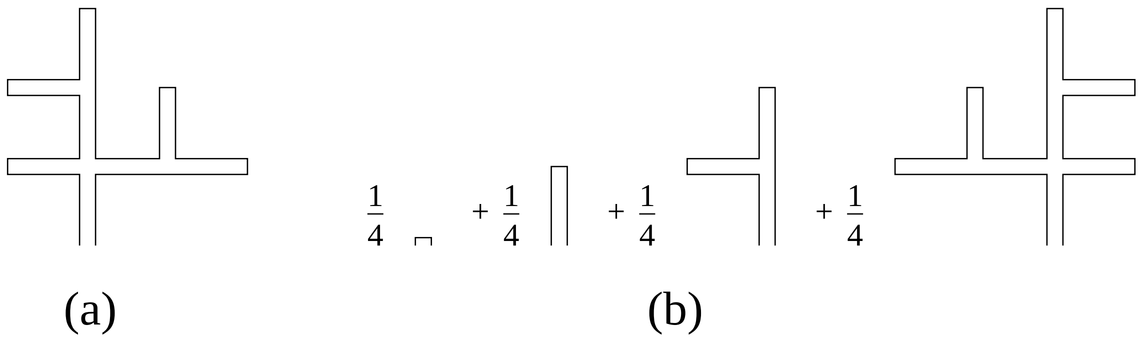

Figure 4: *(a) An example of a true 4-tree. (b) A free 4-tree corresponds to a true N-tree for N = 1,2,3,4, each with probability 1/4, as schematically indicated in this figure.*

momentum for each emitted gluon. The $k_\perp$ is measured with respect to the emitting parent parton, which within the leading log approximation agrees with the transverse momentum in the local dipole rest frame. The azimuth angles are not fixed by the diagram and should be chosen randomly.

We note that the masses of any subsystem is directly determined by the distances in the diagram. If the distance along the curve between two adjacent tips i and j is n steps, the corresponding mass s_{ij} is given by $\log(s_{ij}/s_0) = n \cdot \delta y_g$, where s_0 is the mass scale in the model. Thus in fig 3 we have eg $\log(s_{23}/s_0) = 9 \cdot \delta y_g$ and $\log(s_{36}/s_0) = 6 \cdot \delta y_g$. The total length of the diagram, corresponding to the baseline in fig 1c, gives the measure λ defined in eq (9) and thus represents the final hadron multiplicity.

The rapidity step $\delta y_g \sim 2$ is rather large, but this does not imply that there is no structure on smaller scales. A high energy gluon jet contains sub-jets which contain sub-jets etc. For the trees grown from the original straight baseline in fig 3, the distance δy_g corresponds to a separation in rapidity along the original $q\bar{q}$ axis (ie essentially the thrust axis). Each such tree (cf the examples in fig 4) has a lot of branches, where δy_g is the distance along the local jet direction (with a similar substucture within the branches). The *whole tree* is localized approximately inside one unit of δy_g along the the initial $q\bar{q}$ axis. Thus δy_g is a resolution along an abstract color line. Along the original $q\bar{q}$ axis it does not correspond to the resolution size but rather to a correlation length. The jets within this rapidity gap should be regarded as subjets of one original main jet. To always place the main jets exactly in the middle of each rapidity bin is an approximation, and to reproduce detailed experimental data some smearing has to be introduced. How to translate the diagrams to actual parton momenta will be discussed in more detail in section 6. We want to stress however, that the main objective of this paper is to provide a better understanding of the qualitative features of the parton cascades.

5 Analytic properties

5.1 The Master Equation for the Multiplicities and the λ-measure

We will start with the master equation for the multiplicity generating functions. Let $p_N(n)$ be the probability to obtain just n gluons emitted in a free N-tree and $\mathcal{N}(N)$ the corresponding largest multiplicity. We introduce the generating function $\mathcal{P}_N(z)$ for this distribution

$$\mathcal{P}_N(z) = \sum_{n=0}^{\mathcal{N}(N)} p_N(n) z^n \tag{23}$$

and a corresponding generating function $\mathcal{Q}_N(z)$ for a true N-tree. The functions $\mathcal{P}_N$ and $\mathcal{Q}_N$ are connected by the relation

$$\mathcal{P}_N = \frac{1}{N} \sum_{M=1}^{N} \mathcal{Q}_M \tag{24}$$

which implies the recursive relation

$$\mathcal{Q}_N(z) = N\mathcal{P}_N(z) - (N-1)\mathcal{P}_{N-1}(z) \tag{25}$$

The generating functions must also satisfy the relation

$$\mathcal{Q}_{N+1} = \mathcal{P}_N^2 \mathcal{Q}_N \tag{26}$$

with the boundary conditions

$$\begin{aligned} \mathcal{Q}_1 &= 1, \qquad \mathcal{Q}_2 = z \\ \mathcal{P}_1 &= 1, \qquad \mathcal{P}_2 = \frac{(1+z)}{2} \end{aligned} \tag{27}$$

Eq (26) comes from the fact that a true $(N+1)$-tree differs from a true N-tree by the addition of two free N-"branches". The two recursion relations (25) and (26) obviously determine the functions $\mathcal{P}_N$ and $\mathcal{Q}_N$ for all N.

Eq (26) can be written in the form

$$\log \mathcal{Q}_{N+1} - \log \mathcal{Q}_N = 2 \log \mathcal{P}_N \tag{28}$$

and we note that eqs (26) and (28) are discretised versions of the eqs (15) and (16) in ref [8] (cf also the eqs (5.67) in ref [12] and ref [14]). (The functions $\tilde{P}$ and R in ref [8] correspond essentially to our $\mathcal{Q}$ and $\log \mathcal{P}$ and the Laplace-transforms correspond to the expansion in z^n.)

Actually we may easily generalise the master equation for the gluon multiplicities to the corresponding relations for the distributions in the λ-measure. As discussed above this corresponds to the total length of the curve in fig 3 and is then given by $\lambda = l \cdot \delta y_g$, with l an integer. We may then for a given free N-tree again define the generating function for the distribution in l, $\mathcal{P}_N^{(\lambda)}(\zeta) = \sum p_N^{(\lambda)}(l)\zeta^l$, (where $p_N^{(\lambda)}(l)$ is the probability to have $\lambda = l \cdot \delta y_g$) and we may do the same for a true N-tree, $\mathcal{Q}_N^{(\lambda)}(\zeta)$. Similarly we may define the corresponding combined generating functions in z (for the multiplicities) and in ζ (for the λ measure), $\mathcal{P}_N(z,\zeta)$ and $\mathcal{Q}_N(z,\zeta)$.

It is straightforward to prove that the generating functions, containing also the λ-measure, will fulfil the master equation:

$$\mathcal{Q}_{N+1}(z,\zeta) = \zeta^2 \mathcal{P}_N^2(z,\zeta)\mathcal{Q}_N(z,\zeta) \tag{29}$$

as well as the eq (25). This result stems from the fact that besides the two N-"branches", the function $\mathcal{Q}_N$ also gets a λ contribution $2 \cdot \delta y_g$ from a two-sided addition of (δy_g) in height. Thus with the rescaling $\zeta \mathcal{P}_N(z,\zeta) \to \mathcal{P}_N(z,\zeta)$ *all the recurrence relations are the same*, ie. only the boundary values for $N = 1, 2$ are different when we study the distribution in n, in λ or in the combined distribution in n and λ. In particular for the last case we find (after this rescaling) $\mathcal{P}_1 = \zeta, \mathcal{P}_2 = \zeta(1+\zeta^2 z)/2$.

If we only count gluons with $\log(k_\perp^2) \geq \kappa_{cut} = k \cdot 2\delta y_g$ (where k is an integer), it corresponds to studying the event with a coarser resolution (cf [15] and [11]). It also corresponds to cutting the surface in fig 1c at a height given by $\kappa = \kappa_c$. In this case the equations are still the same, but the boundary values are changed. Since we have no (resolved) gluons for $N \leq k+1$ we obtain $\mathcal{P}_{k+1} = \zeta, \mathcal{P}_{k+2} = \zeta(1+k+\zeta^2 z)/(k+2)$

5.2 The Average Multiplicity and The Dispersion

It is straightforward to write down recurrence relations for the multiplicity moments (as well as for the moments in λ). We note that the derivatives of the distributions $\log(\mathcal{P}_N)$ and $\log(\mathcal{Q}_N)$ evaluated at $z = 1$ $(\zeta = 1)$ will produce the central moments, the $\log(z)$-derivatives

$< n >$, $D^2 =< (n- < n >)^2 >$ (the $\log(\zeta)$-derivatives $< l >$, $< (l- < l >)^2 >$ with $\lambda = l \cdot \delta y_g$), cf subsection 5.3. Finally the combined derivatives provide the correlations between n and l. For a free N-tree we obtain by straightforward manipulations for eg the first two multiplicity moments:

$$
\begin{aligned}
\bar{n}_{N+1} - 2\bar{n}_N + \bar{n}_{N-1} &= \frac{1}{N+1} \cdot 2\bar{n}_{N-1} \\
D^2_{N+1} - 2D^2_N + D^2_{N-1} &= \frac{1}{N+1}(2D^2_{N-1} + 2N(\bar{n}^2_N - \frac{N-1}{N+1}\bar{n}^2_{N-1}))
\end{aligned}
\tag{30}
$$

where $\bar{n}_N$ is the average gluon multiplicity for a free N-tree. Counting only gluons with $\kappa \geq \delta y_g$, as described above, we get for the reduced resolution the boundary values $\bar{n}_{k+1} = 0, \bar{n}_{k+2} = 1/(k+2), D^2_{k+1} = 0, D^2_{k+2} = 1/(k+2)^2$. The same equations are easily found to be valid for $< l >_N +1$, $< (l- < l >)^2 >_N$.

Let us study the multiplicity distribution for an e^+e^--ann. event with $\log(s) = L \cdot \delta y_g$, with L an integer. It is easy to realize that if L is an odd integer the right and left halfs of the curve in fig 3 correspond just to the two sides of a true tree. This implies

$$
\mathcal{P}_L^{e^+e^-} = \mathcal{Q}_{(L+3)/2} \quad , L \text{ odd} \tag{31}
$$

To be exact this gives the distribution in the number of gluons+1, which equals the number of dipoles in the e^+e^--ann. event. Similarly the λ-measure for e^+e^--ann. is one unit (δy_g) less than the result obtained from the $\mathcal{Q}_N$-distribution.

For L even we get also a contribution from the central tree which implies

$$
\mathcal{P}_L^{e^+e^-} = \mathcal{Q}_{(L+2)/2} \cdot \mathcal{P}_{(L+2)/2} \quad , L \text{ even} \tag{32}
$$

From these relations we can easily obtain relations for the average multiplicity or higher multiplicity moments. For the average dipole multiplicity we get

$$
\bar{n}_{L+2} - 2\bar{n}_L + \bar{n}_{L-2} = \frac{2}{L+3}(\bar{n}_L + \bar{n}_{L-2}) \quad , \text{L odd} \tag{33}
$$

and a similar result for L even.

These results may be compared to those obtained in the continuous limit in [8] and [14] (cf also [12]). In the Leading Log Approximation (LLA) and Modified Leading Log Approximation (MLLA) we have for the average multiplicity (in MLLA we here do not include the effect of the process $g \to q\bar{q}$ or colorsuppressed terms)

$$
\frac{d^2\bar{n}}{d\tilde{L}^2} = \bar{\alpha}(\tilde{L}) \cdot \bar{n}(\tilde{L}), \text{ in LLA} \tag{34}
$$

$$
\frac{d^2\bar{n}}{d\tilde{L}^2} = \bar{\alpha}(\tilde{L} - \delta y_g) \cdot \bar{n}(\tilde{L} - \delta y_g), \text{ in MLLA} \tag{35}
$$

where $\tilde{L} = \log(s/s_0)$. We note that the systematic corrections in going from LLA to MLLA (which correspond to corrections stemming from the size of the phase space and nonleading terms in the splitting functions) work in the same way as for the Discrete QCD version.

It is possible to write out the explicit solutions of the equations but we prefer to exhibit the results for the average multiplicity in fig 5a and for the ratio $D^2/ < n >^2$ in fig 5b. We also note that the correlation between l and n is strong in the model and we obtain as seen in fig 5c, that the average values behave for large values of N as $< l > \simeq 3.5 < n >$.

The results presented above describe the dependence upon the total energy for fixed resolution. It is also possible to study the dependence on the resolution scale (specified by the integer k) for fixed energy. If we consider the change $k \to (k-1)$ for fixed N, we note that the generating functions (for $N \geq k+3$) for n and l only depend upon the two boundary value functions $\mathcal{P}_{k+1}$ and $\mathcal{P}_{k+2}$. Thus "the step" $k \to (k-1)$ only changes their dependences on z and ζ:

$$\begin{aligned} \mathcal{P}_{k+1} &= \zeta \to \zeta(k + \zeta^2 z)/(k+1) \\ \mathcal{P}_{k+2} &= \zeta(1 + k + \zeta^2 z)/(k+2) \to \mathcal{P}_{k+1}(1 + k + \zeta^3 z \mathcal{P}_{k+1})/(k+2) \end{aligned} \tag{36}$$

In this way we are led to the system of difference equations

$$l_{[k]} - l_{[k-1]} = -2n_{[k-1]} \tag{37}$$

$$n_{[k]} - n_{[k-1]} = -(l_{[k]} + 1 - n_{[k]})/(k+1) \tag{38}$$

where we have used the notation $n_{[k]}$ for the average multiplicity at the resolution power k for any $N > k+2$, etc. If these are combined we may write the second order difference equation (valid for the same N-values)

$$n_{[k]} - 2n_{[k-1]} + n_{[k-2]} = 2n_{[k-1]}/k \tag{39}$$

and there is a corresponding one for the l-averages. These relations are equivalent to the results obtained in refs [11], [14] and [15] for the continuous case.

5.3 The Zeroes of the Generating Function

We start by noting that as the multiplicity generating function $\mathcal{P}_N$ (in eq 23) is a finite polynomial of degree $\mathcal{N}(N)$ in z, then $\mathcal{P}_{(N+1)}$ will from eq (26) be a polynomial of degree $\mathcal{N}(N+1) = 3\mathcal{N}(N)$ (for $N > 2$). Thus we find that

$$\mathcal{N}(N) = 3^{N-2} \tag{40}$$

In practice this means that if we consider the zeroes, $z_j(N)$, of the generating function, ie we write

$$\mathcal{P}_N = A_N \prod (z - z_j(N)) \tag{41}$$

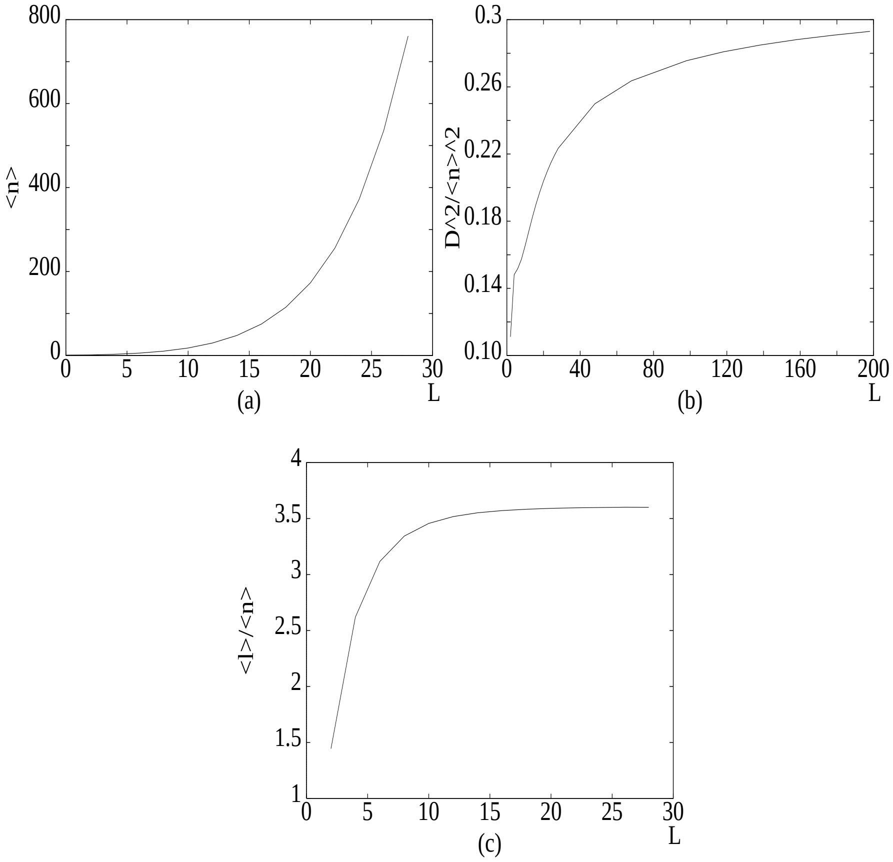

Figure 5: *Some distributions for the dipole multiplicity (=gluon multiplicity+1) and the λ-measure corresponding to e^+e^--events with the energy given by $s = s_0 \cdot e^{L \cdot \delta y_g}$:*
(a) The average dipole multiplicity. (b) The ratio $D^2/ < n >^2$ for the dipole multiplicity.
(c) The ratio $< l > / < n >$, where $l = \lambda/\delta y_g$.

then every $z_j(N)$ "splits up" into three at the $(N+1)$st level. It is a surprising fact that *all of the roots gather around a finite "curve"* in the complex z-plane. This "curve" will in the large N-limit correspond to the region of singularities for the limiting function $\mathcal{P}_{N\to\infty}$. In this subsection we will briefly consider some of the properties.

The reason to consider these zeroes is the already mentioned relationship between the moments of the distributions and an expansion around $z = 1$ of the logarithm of the generating function:

$$\begin{aligned}
\log(\mathcal{P}_N(z)) &= \log(A_N) + \sum(z - z_j(N)) \qquad (42)\\
\sum n p_N(n) &= < n >= \frac{d\log(\mathcal{P}_N)}{dz}(z=1) = \sum \frac{1}{1-z_j}\\
< (n- < n >)^2 > - < n > &= \frac{d^2\log(\mathcal{P}_N)}{dz^2}(z=1) = -\sum \frac{1}{(1-z_j(N))^2}
\end{aligned}$$

We note that due to eq (26) all the zeroes of the $\mathcal{P}_K$, $K < N$ also occur for $\mathcal{P}_N$ because we may write

$$\mathcal{P}_N(z) = \prod_{j=2}^{N} q_j(z) \tag{43}$$

$$q_2(z) = \mathcal{P}_2(z)$$

$$q_N(z) = \frac{1}{N} \cdot (N - 1 + z q_2^{2N-5} q_3^{2N-7} \cdots q_{N-1}) \tag{44}$$

and we note that the degree of the polynomial q_N is $2 \cdot 3^{N-3}$, while the remaining powers in eq (40) stem from the polynomials $q_K, \ K < N$.

As both $\mathcal{P}_N$ and q_N are polynomials they are, as well as their logarithms, analytic functions of z. This implies that the real and the imaginary parts of the logarithms in particular are solutions to the two-dimensional Laplace equation with the coordinates (x, y), the real and imaginary parts of $z = x + iy$. The real part of the logarithms of the generating functions can be interpreted as a potential function in two-dimensional electrostatics stemming from unit charges placed at the zeroes of the corresponding polynomials.

In fig 6 we show the behaviour of the zeroes for the polynomials $q_N, \ N \leq 6$ and in order to see the emerging structures more in detail we show in fig 7 the results in a small sector of the emerging curve. The zeroes constitute a Julia set and form a fractal curve in the complex plane. A proper interpretation of this curve is however still missing.

6 The Energy Momentum Vectors of the Emitted Gluons

In this section we want to use Discrete QCD to generate actual events, and demonstrate that the model does reproduce the essential features of the gluon cascades. For this we need a translation from the abstract picture in fig 3 to the space of the energy momentum vectors of the emitted gluons and the recoiling $(q, \bar{q})$-particles.

One problem is to take into account *the necessary recoils*, ie the fact that when a gluon is emitted from a dipole then the two "original" partons constituting the dipole will have to take up the changes in energy-momentum. From ref [6] we know that different possible recoil strategies provide basically the same results. (As we do not know the next order in the matrix element calculations we can at present only guess the best approximation to take up the recoils.) For definiteness we use the recoil strategy to minimise the transverse momenta of the "emitting" partons with respect to the original dipole axis in the cms of the dipole, cf [6] (where also the the flat distribution in the azimuthal angle is applied).

We should also take into account the fact that the proper phase space in eq (5) does not fill all

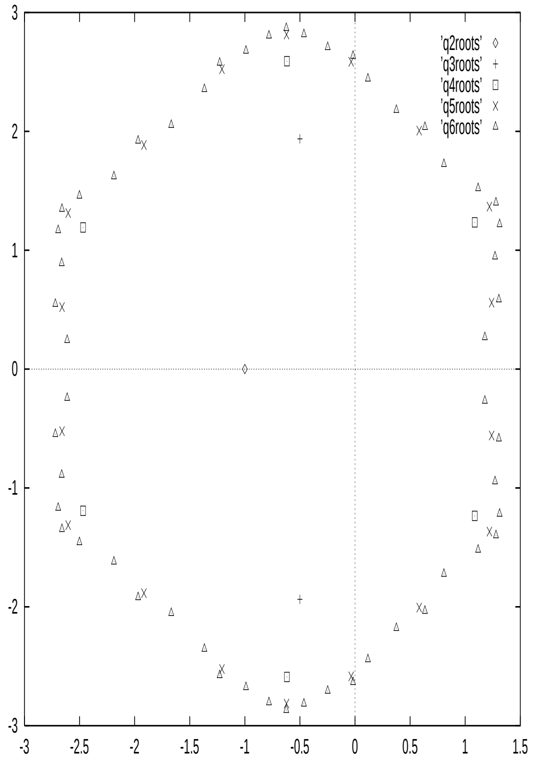

Figure 6: *The roots to the polynomials* q_N, $N = 2, ..., 6$.

of the triangle in fig 1. In addition nonleading terms in the splitting functions suppress hard emissions close to the kinematic limits. As mentioned in section 4, it turns out that both of these corrections can be taken into account just by cutting away a strip of the size $\delta y_g/2$ along the edges of each of the triangles which are the basic parts of the emission phase space, ref [14]. The fact that the two effects are compensated by the same procedure is a nice coincidence.

We will then simply produce an "abstract state" according to the probabilities given above. For a state with the base line $L \cdot \delta y_g$, the possible emission positions for the background triangle are shown in the in fig 8a. After the emissions in the background triangle we repeat the procedure for the new triangles.

After that we use the DCM prescription and look for the largest $k_\perp$ (anywhere in the state) and consider that as "the first" emitted gluon, thereby producing "the first" two dipoles with their logarithmic mass squares defined by the position of the gluon. An emitted gluon is then placed at the centre of each phase space cell (cf below, however for the hardest gluons). We provide an azimuthal angle stochastically from a flat distribution, thereby defining all properties of the state after "the first" emission (besides a general mass scale). Then we repeat the procedure, finding "the second" emitted gluon etc.

There is one place where we need to be a bit more careful, *viz* when we emit a very hard gluon close to the phase space boundary. One effective gluon represents the total activity in one phase space cell in the $(\log k_\perp^2, y)$-plane. To always put it exactly in the centre of the cell of

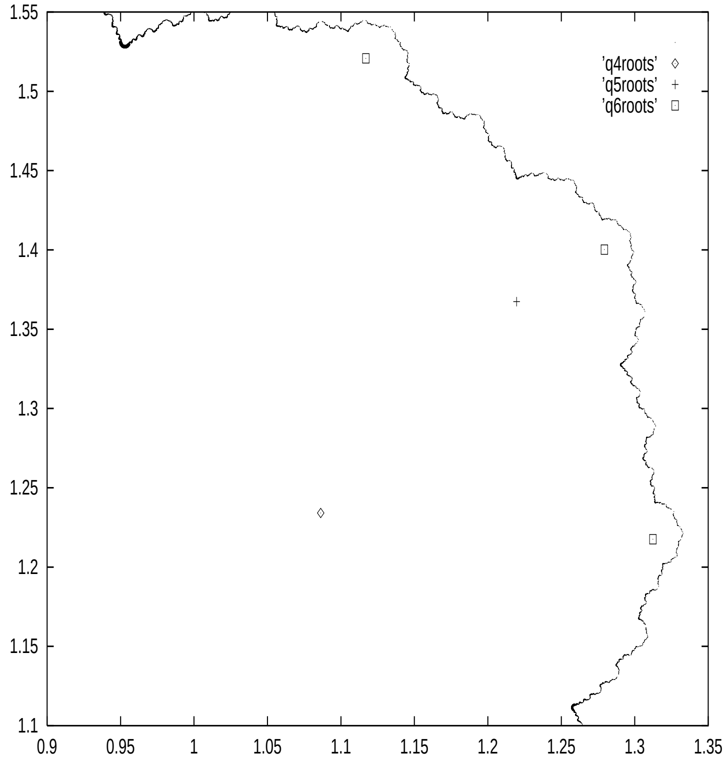

Figure 7: *A small part of the curve that connects the roots to q_N, $N \to \infty$. For comparison, some roots to the polynomials when N is small, are also shown.*

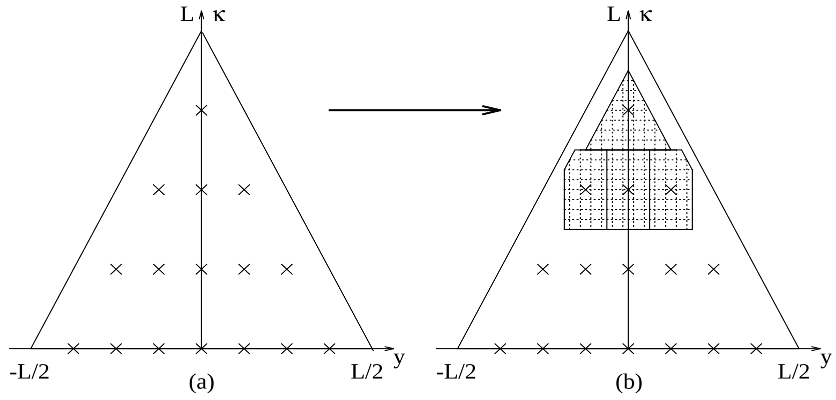

Figure 8: *(a) After cutting away a strip $\delta y_g/2$ on each edge of the triangle there are only interior emission points left. (b) The "smoothing" procedure: with a uniform distribution the hardest gluons are allowed to be emitted anywhere inside the marked boxes.*

course gives a very spiky result and a more realistic description can be obtained with a smoother distribution within the cell. From experience with MC simulation for e^+e^--annihilation we know that the result is very sensitive to the treatment of the hardest gluon, while the softer gluons are much less important. Naturally the distribution must also be kept within the kinematic limits. In case there is a gluon in the cell with highest $k_\perp$ we distribute it evenly within the triangle indicated in fig 8b, where we have cut away strips along the sides where the emission,

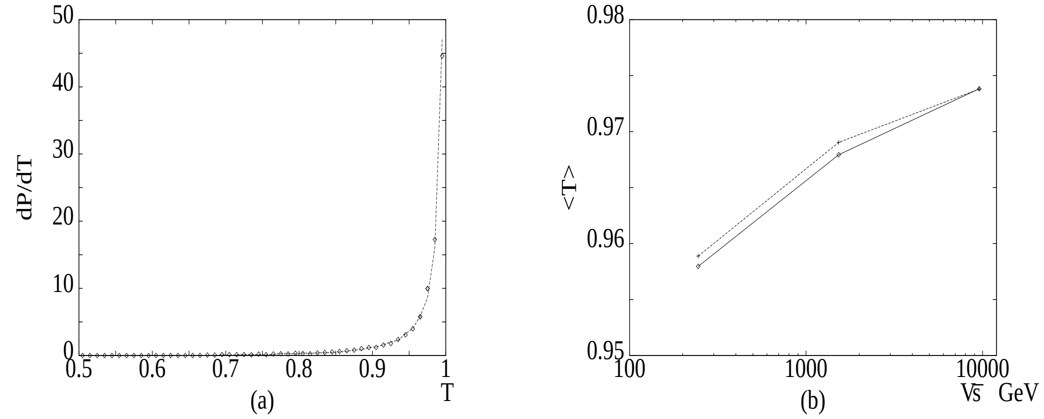

Figure 9: *(a) Comparison for the thrust distribution between ARIADNE (dashed line) and the discrete Monte Carlo (points) at the energy 1531 GeV, corresponding to a triangle base line of length* $8 \cdot \delta y_g$. *(b) Average for the thrust as a function of the cms energy* $\sqrt{s}$. *ARIADNE produces the points connected by the dashed (upper) line and the discrete Monte Carlo the points connected by the solid (lower) line.*

as discussed above, is either forbidden or suppressed. Also at the second highest level we choose a smooth distribution (see fig 8b), while for the softer gluons we are satisfied by always putting them in the centre of the corresponding cell.

Before comparing with experiments we must also fix the single parameter in the model, the mass scale $\Lambda_{discrete}$, defined such that

$$s = \Lambda^2_{discrete} \cdot exp(L \cdot \delta y_g) \tag{45}$$

with L an integer. Naturally $\Lambda_{discrete}$ does not have to coincide with eg $\Lambda_{\overline{MS}}$ or the Λ-value used in other cascade models. We do this by studying how the λ-measure in eq (9) varies with energy and adjust the mass scale so that our discrete model gives the same result as the ARIADNE MC (which is known to reproduce data well). The definition of the λ-measure in eq (9) is unstable against the emission of soft or collinear gluons. This is not a problem in discrete QCD, where all the effective gluons are well separated. In the ARIADNE MC there is however a weaker cutoff for soft or collinear gluons and for a comparison it is important that we use the infrared generalisation of the λ-measure discussed in refs [9] and [16]. In doing so, we find very good agreement between $< \lambda >_{discrete}$ and $< \lambda >_{ARIADNE}$ for $\Lambda_{discrete} \approx 1\text{GeV}$.

We now have a MC which can be used for comparison with experiments. As an example we show in fig 9 results for the thrust variable T compared with results from ARIADNE.

7 Conclusions

We have developed a new approximation scheme for perturbative QCD cascades. The phase space is divided into cells in which all emission is represented by one "effective gluon". The size of the cells is related to the properties of the running coupling constant and it is rather large, which implies that we have only few effective gluons. Simple recursion relations are obtained for the gluon multiplicity and for the hadron multiplcity as represented by the λ-measure from ref [8]. The relations are discretised versions of the differential equations obtained in LLA and MLLA for the continuous case.

Since the multiplicity of effective gluons is limited, the generating functions for the multiplicity distributions are simple polynomials. Thus the properties of the distributions are determined by the zeroes of these polynomials, which for high energies constitute a fractal curve.

We have also developed a simple MC generating hadronic final states and the results are very similar to conventional MC programs.

We conclude that this discretised version of QCD, with a limited number of gluon emissions, seems to contain the essential properties of QCD cascades. In particular we want to stress that it presents a dynamical cutoff for soft emissions and we want to study the properties of this cutoff and applications to DIS in future works.

References

[1] T. Sjöstrand and M. Bengtsson, Comput. Phys. Commun. 43 (1987) 367

[2] L. Lönnblad, Comput. Phys. Commun. 71 (1992) 15

[3] G. Marchesini and B.R. Webber, Nucl. Phys. B310 (1988) 461

[4] E. de Wolf, private communication

[5] Ya.I. Azimov, Yu.L. Dokshitzer, V.A. Khoze, and S.I. Troyan, Phys. Lett. B165 (1985) 147

[6] B. Andersson, G. Gustafson and C. Sjögren, Nucl. Phys. B380 (1992) 391

[7] G. Gustafson, Phys. Lett. B175 (1986) 453;
G. Gustafson and U. Pettersson, Nucl. Phys. B306 (1988) 746

[8] B. Andersson, P. Dahlqvist and G. Gustafson, Phys. Lett. B214 (1988) 604

[9] B. Andersson, P. Dahlqvist and G. Gustafson, Z. Phys. C44 (1989) 455

[10] B. Andersson, P. Dahlqvist and G. Gustafson, Nucl. Phys. B328 (1989) 76

[11] G. Gustafson, A. Nilsson, Nucl. Phys. B355 (1991) 106;
G. Gustafson, A. Nilsson, Z. Phys. C52 (1991) 533

[12] For a review, see Yu.L. Dokshitzer, V.A. Khoze, A.H. Mueller and S.I. Troyan, Basics of Perturbative QCD (Editions Frontières, Gif-sur-Yvette, 1991)

[13] S. Coleman, Aspects of symmetry (Cambridge University Press, 1985)

[14] G. Gustafson, Nucl. Phys. B392 (1993) 251;
M. Olsson and G. Gustafson, Nucl. Phys. B406 (1993) 293

[15] B. Andersson, Nucl. Phys. B360 (1991) 109

[16] B. Andersson, G. Gustafson and B. Söderberg, Nucl. Phys.B264 (1986) 29